Received power modelling in ultra-dense networks

Danaisy Prado-Alvarez,[1,✉] Alejandro Antón,[1] Daniel Calabuig,[1] Jose F. Monserrat,[1] Samer Bazzi,[2] and Wen Xu[2]

[1] *iTEAM Research Institute, Universitat Politècnica de València, Valencia, Spain*

[2] *Advanced Wireless Technology Laboratory, Huawei Technologies Duesseldorf GmbH, Munich, Germany*

✉Email: dapraal@upv.edu.es

In received power modelling for system level simulations, the relative orientation of the transmitter and receiver antennas are not generally considered. By doing that, a constant gain of the receiver antenna, independently of the angle of arrival, is implicitly assumed. This is usually of minor relevance for small or low-dense scenarios. However, in ultra-dense deployments, especially those based on cell-free massive multiple-input–multiple-output architectures where users interact with all access points, the consideration of the antennas relative orientation comes to the forefront. In this paper, the impact of whether to take the receiver antenna gain into account or not for ultra-dense indoor environments with ceiling-mounted antennas are studied. A simple approach to take this gain into account using the antenna effective area is provided. Finally, this approach is compared with that based on antenna radiation patterns.

Introduction: In response to the high capacity demand of future communication systems, the deployment of ultra-dense networks with a massive number of antennas has emerged as a potential solution [1]. In this context, cell-free massive multiple-input–multiple-output (MIMO) has been defined as an implementation of massive MIMO in an ultra-dense network with a considerably higher amount of access points (APs) than user equipmets (UE). The APs are distributed over a wide area, and connected to a single central processing (CPU) via front-haul, which controls network synchronisation, power allocation, data throughput etc. Each AP and UE can have one or more antennas [2]. The user-centric vision of cell-free massive MIMO [3], guarantees that the UE connects to a certain number of the surrounding APs, or to all of them in the case of canonical cell-free massive MIMO [4]. The cell-free massive MIMO systems fundamentals have been described in several works, e.g. in refs. [2, 4–6].

Generally, in the modelling of small cells (SC) deployments or even of cell-free massive MIMO, as in refs. [7, 8], the relative orientation of the transmitter and receiver antennas is not considered. This is equivalent to assuming (i) a constant gain of the receiver antennas in all directions, or (ii) that the receiver antennas orientation depends on the position of the transmitter in such a way that the direction of arrival is always the same. However, although the error generated by this assumption is acceptable in some cases, the same is not valid for ultra-dense deployments when the total signal/interference received by all or a large number of APs or UE is considered. In fact, we will show that, with the assumption that the direction of arrival is always the same, some APs partially block the transmitted signal to other APs in the uplink of sufficiently large ultra-dense scenarios.

This work addresses the modelling of received power for ultra-dense systems, specifically, for the uplink of cell-free massive MIMO in indoor environments with ceiling-mounted APs. Our main objective is to raise awareness of the implications of not considering the transmitter and receiver antennas orientation in such systems, which results in a significant overestimation of the received power. In this regard, an approach is proposed to consider the effective area of the receiver antenna. Finally, a comparison is done with the approach considering the radiation pattern of the receiver antenna.

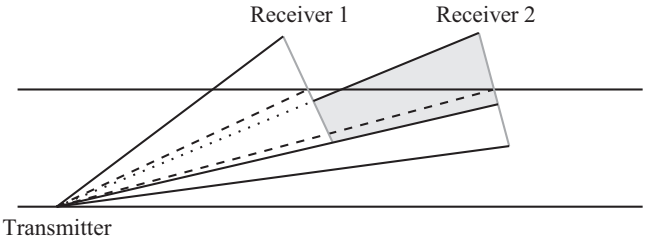

Fig. 1 *Shadow effect of Receiver 1 onto Receiver 2, for perfectly oriented receivers towards the transmitter*

Problem statement: For the sake of clarity, the received power model is firstly introduced. According to Friis free space propagation model [9], the received power, P_r, can be calculated as

$$P_r = \frac{P_t G_t G_r}{\left(\frac{4\pi d}{\lambda}\right)^2}, \tag{1}$$

where P_t is the transmitted power, G_t is the gain in transmission, G_r is the gain in reception, d is the distance between transmitter and receiver, and λ is the wavelength.

It is worth noting that G_t and G_r depend on the relative orientation of the transmitter and receiver antennas [9]. This implies that P_r depends not only on the transmitter and receiver distance, but also on the angular orientation of the antennas. Note that the pathloss models do not include the effect of the antennas orientation, see, e.g. Tables A1 and A2 in ref. [10]. Therefore, for system level simulations, it is important to include the effect of the antennas orientation in addition to the pathloss model. However, this is not generally done in most of the research works. In this case, the product $G_t G_r$ is assumed constant, which is equivalent to assume that the relative antennas orientation is fixed. In the case of the uplink of cell-free massive MIMO, this assumption implies that the APs antennas should rotate depending on the distance to the UE. However, if APs are closely deployed, and relatively far APs are considered for the received signal power computation, it is easy to find APs which orientation produce a shadow onto further APs (not related to shadowing modelled by the slow fading). This effect is depicted in Figure 1. As a consequence, Receiver 2 in Figure 1 cannot actually receive all the power defined in Equation (1), which in turn leads to an overestimated received power.

Towards obtaining a more realistic model, the antennas should be considered parallel to the ceiling and then, the corresponding fraction of the received power should be modelled. In the next sections, we analyse two approaches with $G_t = 1$ and different models for G_r. The first one considers the radiation pattern of the receiver antennas, and the second one takes the effective area of the receiver antennas into account.

Radiation pattern approach: The radiation pattern approach consists of the modelling of G_r as a function of the angle of arrival of the signal, θ, as it is shown in ref. [10]. $G_r(\theta)$ takes values such that for $|\theta_1| \leq |\theta_2|$, $G_r(\theta_1) \geq G_r(\theta_2)$. With this radiation pattern, if the receiver antennas are fixed to the ceiling in an indoor scenario, and the beam is steered to the ground, i.e. $\theta = 0$ corresponds to the direction perpendicular to the ground, the maximum gain is achieved below the antennas, and this gain becomes smaller as the distance to the antenna increases until it reaches the minimum gain. This is because θ increases with the distance.

Effective area approach: In this section, we present another approach to include, in the system model, a variable gain in reception with respect to the angle of arrival. In particular, we propose to integrate the effective area [9] into the pathloss model. The effective area is modelled at the receiver as the projection of the physical area in the direction of the transmitter (see Figure 2).

Mathematically, A_e can be derived through the following equations:

$$\sin\alpha = \frac{h_r - h_t}{d} = \frac{A_e}{A}, \tag{2}$$

$$A_e = A\frac{h_r - h_t}{d}, \; h_r > h_t, \tag{3}$$

where $\alpha = \frac{\pi}{2} - \theta$ is the angle of departure from the transmitter with respect to the floor's normal, h_t and h_r are the heights of the transmitter and

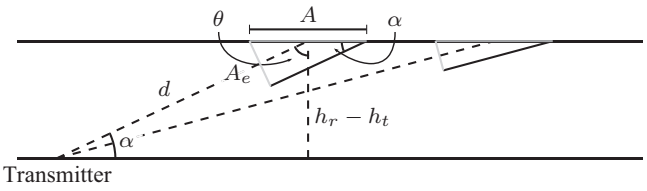

Fig. 2 *Cross-section of a scenario with one transmitter and two receivers and representation of the effective area*

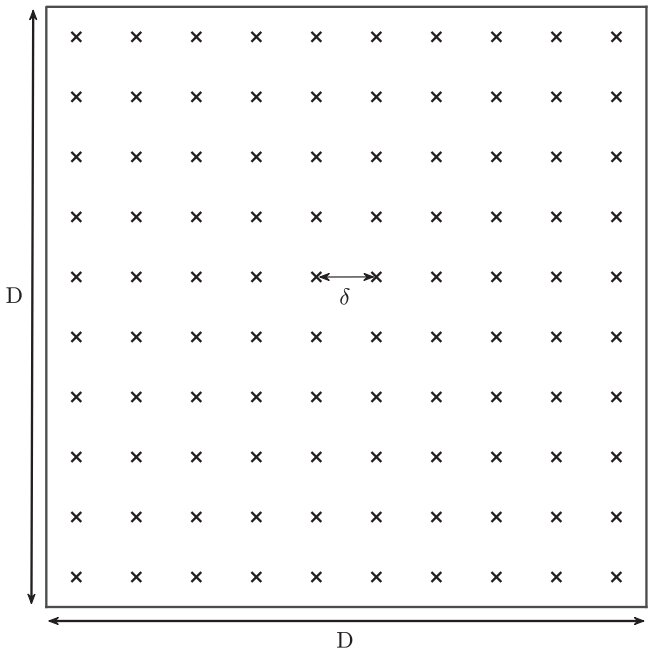

Fig. 4 *Scenario layout for $D = 50$ m and $\delta = 5$ m*

receiver respectively, d is the distance between them, and A is the physical area of the receiver antenna. Then, the gain at the receiver antenna can be computed as

$$G_{\mathrm{r}} = \frac{A_{\mathrm{e}}}{A} = \frac{h_{\mathrm{r}} - h_{\mathrm{t}}}{d}. \tag{4}$$

Finally, using Equation (4), Equation (1) can be expressed as

$$P_{\mathrm{r}} = \frac{P_{\mathrm{t}} G_{\mathrm{t}}}{\left(\frac{4\pi}{\lambda}\right)^2 d^3} (h_{\mathrm{r}} - h_{\mathrm{t}}). \tag{5}$$

Comparing Equation (5) with Equation (1), it can be noticed that, in Equation (5), we replace G_{r} by a constant, $h_{\mathrm{r}} - h_{\mathrm{t}}$, and an increase by 1 of the distance exponent. Therefore, with this approach, G_{r} can be easily included in the pathloss model.

Alternatives comparision: In order to analyse qualitatively and quantitatively the effect of considering G_{r}, the following evaluation scenario is proposed. The scenario consists of a squared scenario where a network of APs is installed on the ceiling. The APs are equi-spaced with an intersite distance $\delta = 5$ m. Additionally, there is one UE in the centre of the scenario transmitting to all APs at the same time with P_{t} equal to 21 dBm. The heights are 6 m and 1.5 m for the APs and the UE respectively. These heights are typical for indoor industrial scenarios as stated in refs. [8, 11]. The evaluation is carried out for different scenario dimensions ranging from a 10×10 m^2 up to $10{,}000\times10{,}000$ m^2, while δ remains fixed. Consequently, the number of APs grow with the scenario size. The scenario side length is denoted as D, as it can be seen in Figure 4.

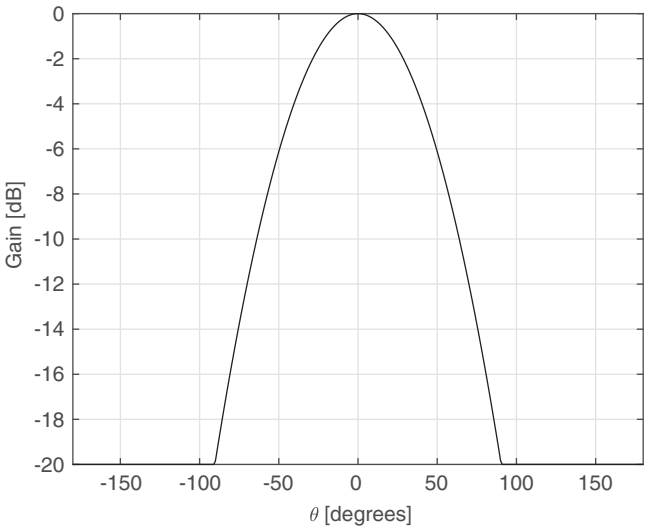

Fig. 3 *Radiation pattern*

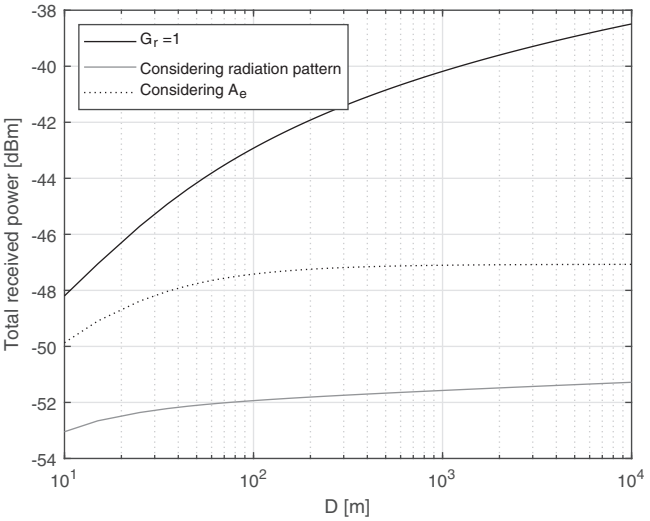

Fig. 5 *Total received power for all alternatives*

For the radiation pattern alternative, we model $G_{\mathrm{r}}(\theta)$ with the antenna element radiation pattern used in ref. [10], without considering any tilt. Thus, the receiving antenna gain is modelled as

$$G_r(\theta) = -\min\left[12\left(\frac{\theta}{\theta_{3\mathrm{dB}}}\right)^2, G_{r_{\mathrm{m}}}\right], \tag{6}$$

where $\theta_{3\mathrm{dB}}$ is the beam width of the radiation pattern and $G_{r_{\mathrm{m}}}$ is the maximum attenuation. Following the typical case used in ref. [10], $\theta_{3\mathrm{dB}}$ is assumed to equal 70 degrees and $G_{r_{\mathrm{m}}} = 20$ dB. Figure 3 shows the radiation pattern.

In this work, the pathloss model for free space based on the Friis equation has been considered. Therefore, it is possible to study the modelling of the received power avoiding to consider other effects of different nature that are taken into account when obtaining the empirical models. The evaluation is carried out in uplink, i.e. in this case the transmitting antenna is the UE's antenna and the receiving antennas are those of the APs.

Figure 5 presents three curves which show how the total received power at the APs increases with the size of the scenario when considering $G_{\mathrm{r}} = 1$, the radiation pattern or A_{e}. As it can be observed, the total received power for $G_{\mathrm{r}} = 1$ noticeably increases even for scenarios as large as $10{,}000\times10{,}000$ m^2. Although with a substantially slower growth, the approach that takes into account the radiation pattern also shows an increasing trend. This is due to the consideration of a maximum attenuation of the radiation pattern, specifically 20 dB. In particular, the total received power in this case is greater than that received with a constant

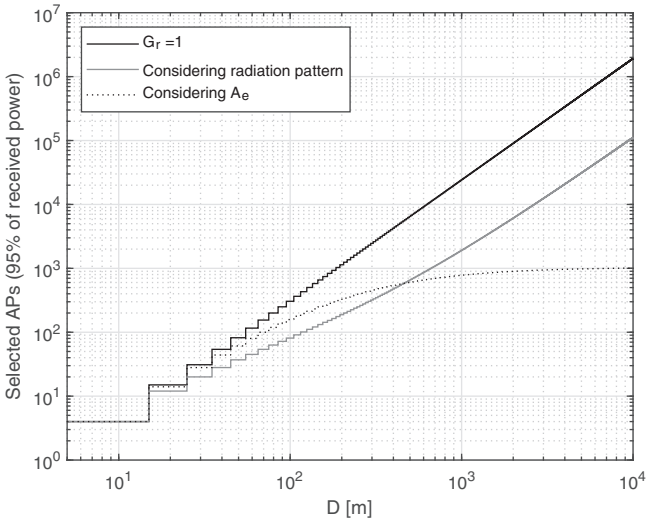

Fig. 6 *Selected APs for all alternatives*

gain of −20 dB. It is worth noting that, although not depicted in Figure 5, the curve corresponding to the received power with a −20 dB constant gain is just a vertical shift of the $G_r = 1$ curve. Therefore, the received power taking into account the radiation pattern in Equation (6) cannot converge if this power does not converge with a constant gain. Finally, for the approach where A_e is considered, from a scenario size of about 100×100 m^2, the curve is practically flat, i.e. the growth of the total received power is imperceptible with increasing scenario side lengths.

To illustrate with another example the consequences of considering one of these approaches, the number of APs where 95% of the power is received is determined for different scenario sizes. A similar criterion has been followed for downlink in ref. [8] to determine the APs that provide the 95% of the power to a particular UE. Figure 6 presents three curves which show how the number of selected APs increases when considering $G_r = 1$, the radiation pattern or A_e. The curves for $G_r = 1$ and for the radiation pattern grow rapidly without reaching a convergence point. On the other hand, the number of selected APs in the case considering A_e tends to flatten out. It is important to note that the behaviour of the approach with the radiation pattern strongly depends on the particular pattern used. In other words, with a different radiation pattern, the selected APs with this approach could differ from that shown in Figure 6. However, if the radiation pattern has a maximum attenuation, the behaviour for high Ds will be similar to that in the figure, independently of the particular pattern used. More specifically, we conclude from Figure 5 that the total received power increases even for large scenarios, and that this is due to the maximum attenuation. As a consequence, and since the 95% of the received power also increases, we need to select more APs to achieve this target.

Analysing the two figures at the same time, it can be concluded that: (i) when considering a constant receiver gain from all directions, the received power and the number of selected APs increase with respect to the size of the scenario, even for sizes of $10{,}000\times10{,}000$ m^2; (ii) for the solution considering the radiation pattern of the receiving antennas in uplink, the total received power grows considerably slower than in the $G_r = 1$ case, although, the number of selected APs exhibits a similar growth; and (iii) when considering the effective area, it is possible to appreciate a stabilisation for both the received power and the number of selected APs.

Conclusions: The fact that the received power is estimated without taking into account the antenna orientation or the effective area of the antennas may lead to an overestimation. In this work, we have analysed both the behaviour of the received power and the number of APs where this power is concentrated for scenarios of different sizes. We compare three approaches: considering a constant receiver gain, considering the radiation pattern of the receiver antennas, and considering the effective area of the receiver antennas. We conclude that the results of the first two approaches are linked if the radiation pattern has a maximum attenuation. In particular, the total received power with the radiation pattern cannot converge for increasing scenario sizes, if this power does not converge with the constant gain. Moreover, we showed that the total received power and the number of APs significantly increase with the scenario size for the first two approaches. The approach that considers the effective area is the only one with a noticeable convergent behaviour. This is an important conclusion, since, in the real world, the received power is clearly upper bounded by the transmitted power. This behaviour is only mimicked by the approach that considers the effective area. As an additional result, we show that the effect of the effective area can be easily integrated in pathloss model.

Acknowledgement: The work of Danaisy Prado was supported by the H2020 Marie Curie Program, with Project Grant No. 766231 WAVECOMBE - ITN - 2017. This was also supported by the Spanish Ministry of Science, Innovation and University under the project RTI2018-099880-B-C31.

Conflict of inetrest: The authors declare no conflict of interest.

Received: *4 February 2022* Accepted: *26 February 2022*
doi: 10.1049/ell2.12470

References

1 Calabuig, D., Barmpounakis, S., Gimenez, S., Kousaridas, A., Lakshmana, T.R., Lorca, J., Lunden, P., Ren, Z., Sroka, P., Ternon, E., Venkatasubramanian, V., Maternia, M.: Resource and mobility management in the network layer of 5G cellular ultra-dense networks. *IEEE Commun. Mag.* **55**(6), 162–169 (2017). https://doi.org/10.1109/MCOM.2017.1600293
2 Ngo, H.Q.: Cell-free massive MIMO. In: Shen X., Lin X., Zhang K. (eds.) *Encyclopedia of Wireless Networks*, pp. 1–6. Springer, Cham (2018)
3 Alonzo, M., Buzzi, S.: Cell-free and user-centric massive MIMO at millimeter wave frequencies. In: 2017 IEEE 28th Annual International Symposium on Personal, Indoor, and Mobile Radio Communications (PIMRC), pp. 1–5. IEEE, Piscataway, NJ (2017)
4 Interdonato, G., Frenger, P., Larsson, E.G.: Scalability aspects of cell-free massive MIMO. In: ICC 2019—2019 IEEE International Conference on Communications (ICC), pp. 1–6. IEEE, Piscataway, NJ (2019)
5 Nayebi, E., Ashikhmin, A., Marzetta, T.L., Yang, H., Rao, B.D.: Precoding and power optimization in cell-free massive MIMO systems. *IEEE Trans. Wireless Commun.* **16**(3), 4445–4459 (2017). https://doi.org/10.1109/twc.2017.2698449
6 Björnson, E., Sanguinetti, L.: Making cell-free massive MIMO competitive with MMSE processing and centralized implementation. *IEEE Trans. Wireless Commun.* **19**(1), 77–90 (2020). https://doi.org/10.1109/TWC.2019.2941478
7 Ngo, H.Q., Ashikhmin, A., Yang, H., Larsson, E.G., Marzetta, T.L.: Cell-free massive MIMO versus small cells. *IEEE Trans. Wireless Commun.* **16**(3), 1834–1850 (2017). https://doi.org/10.1109/twc.2017.2655515
8 Interdonato, G., Björnson, E., Ngo, H.Q., Frenger, P., Larsson, E.G.: Ubiquitous cell-free Massive MIMO communications. *EURASIP J. Wireless Commun. Netw.* **2019**(1), 197 (2019). https://doi.org/10.1186/s13638-019-1507-0
9 Balanis, C.A.: *Antenna Theory: Analysis and Design*. Wiley, Hoboken (2016)
10 Series, M: Guidelines for evaluation of radio interface technologies for IMT-Advanced. *Rep. ITU* **638**, 1–72 (2009)
11 Tanghe, E., Joseph, W., Verloock, L., Martens, L., Capoen, H., Herwegen, K., Vantomme, W.: The industrial indoor channel: large-scale and temporal fading at 900, 2400, and 5200 MHz. *IEEE Trans. Wireless Commun.* **7**(7), 2740–2751 (2008). https://doi.org/10.1109/twc.2008.070143